JOC Article

Macrocyclic Bisbinaphthyl Fluorophores and Their Acyclic Analogues: Signal Amplification and Chiral Recognition

Zi-Bo Li, Jing Lin, Hui-Chang Zhang, Michal Sabat, Marilise Hyacinth, and Lin Pu*

Department of Chemistry, University of Virginia, Charlottesville, Virginia 22904-4319

lp6n@virginia.edu

Received April 15, 2004

A series of optically active macrocyclic and acyclic bisbinaphthyls have been synthesized and characterized. The structure of one of the bisbinaphthyl macrocycles has been established by a single-crystal X-ray analysis. The UV and fluorescence spectra of these chiral compounds in various solvents and at different concentrations are studied. Formation of excimers is observed for the macrocyclic bisbinaphthyl compounds. Introduction of conjugated substituents to the 6,6′-positions of the binaphthyl units in the macrocycles leads to greatly amplified fluorescence signals. Using the 6,6′-substituted bisbinaphthyl macrocycles in place of the unsubstituted macrocycles allows a 2 orders of magnitude reduction in the sensor concentration for the fluorescence measurements. These macrocycles have exhibited highly enantioselective fluorescent enhancements in the presence of chiral α-hydroxycarboxylic acids and N-protected α-amino acids. They are useful as fluorescent sensors for chiral recognition. The macrocycles show much greater enantioselectivity in the substrate recognition than their acyclic analogues.

Introduction

Organic macrocycles have been extensively studied in the host−guest chemistry because of their better organized binding sites than the corresponding acyclic compounds.[1−5] Among many chiral macrocyclic compounds, the 1,1′-binaphthyl-based hosts hold prominent positions in chiral recognition.[1,5a] The 1,1′-binaphthyl macrocycles have exhibited excellent chiral discrimination ability toward organic substrates when analyzed by NMR, UV, and various separation methods. However, prior to our recent work,[6] there was almost no report on using binaphthyl-based macrocycles in fluorescent recognition.[7,8] Fluorescence-based enantioselective sensors[9] are of great practical value because they can potentially provide a real time analytical tool for chiral assay. Rapid determination of the enantiomeric composition of organic compounds will be very useful in the high-throughput combinatorial analysis of chiral drug molecules and catalysts. Because of the excellent chiral recognition properties of binaphthyl macrocycles, we have initiated a program to explore their use as enantioselective fluorescent sensors.

We are interested in the enantioselective fluorescent recognition of chiral carboxylic acids such as α-hydroxycarboxylic acids and α-amino acids.[9,10] These compounds are precursors to as well as the structural units of many important organic compounds. Highly enantioselective fluorescent sensors for these molecules should greatly facilitate the determination of their enantiomeric composition and allow a rapid screening of chiral catalysts or reagents for their synthesis.

We have chosen the 1,1′-binaphthyl macrocycles (*S*)- and (*R*)-**1** (*S* and *R* stand for the configuration of the 1,1′-binaphthyl units), previously prepared by Brunner and Schiessling,[11] in our fluorescent recognition study for the following reasons: (1) These macrocycles contain two

(1) (a) Cram, D. J. *Science* **1988**, *240*, 760−767. (b) Cram, D. *Angew. Chem., Int. Ed. Engl.* **1988**, 27, 1009−1020.

(2) Lehn, J.-M. *Angew. Chem., Int. Ed. Engl.* **1988**, *27*, 89−112.

(3) (a) Constable, E. C. *Coordination Chemistry of Macrocyclic Compounds*; Oxford; Oxford University Press: New York, 1999. (b) Lindoy, L. F. *The Chemistry of Macrocyclic Ligand Complexes*; Cambridge University Press: New York, 1989.

(4) (a) Stoddart, J. F. In *Topics in Stereochemistry*; Eliel, E. L., Wilen, S. H., Eds.; John Wiley & Sons: New York, 1987; Vol. 17, pp 207−288. (b) Still, W. C. *Acc. Chem. Res.* **1996**, *29*, 155−163. (c) Zhang, X. X.; Bradshaw, J. S.; Izatt, R. M. *Chem. Rev.* **1997**, *97*, 3313−3361.

(5) (a) Pu, L. *Chem. Rev.* **1998**, *98*, 2405−2494. (b) Webb, T. H.; Wilcox, C. S. *Chem. Soc. Rev.* **1993**, *22*, 383−395.

(6) Lin, J.; Zhang, H.-C.; Pu, L. *Org. Lett.* **2002**, *4*, 3297−3300.

(7) One report recently appeared on using binaphthyl-based organometallic macrocycles in fluorescent recognition: Lee, S. J.; Lin, W. *J. Am. Chem. Soc.* **2002**, *124*, 4554−4555.

(8) Selected references on using chiral binaphthyl molecules in enantioselective fluorescent discrimination: (a) Irie, M.; Yorozu, T.; Hayashi, K. *J. Am. Chem. Soc.* **1978**, *100*, 2236−2237. (b) Yorozu, T.; Hayashi, K.; Irie, M. *J. Am. Chem. Soc.* **1981**, *103*, 5480−5484. (c) James, T. D.; Sandanayake, K. R. A. S.; Shinkai, S. *Nature* **1995**, *374*, 345−347. (d) Iwanek, W.; Mattay, J. *J. Photochem. Photobiol. A: Chem.* **1992**, *67*, 209−226. (e) Avnir, D.; Wellner, E.; Ottolenghi, M. *J. Am. Chem. Soc.* **1989**, *111*, 2001−2003. (f) Parker, K. S.; Townshend, A.; Bale, S. J. *Anal. Proc.* **1995**, *32*, 329−332. (g) Beer, G.; Rurack, K.; Daub, J. *J. Chem. Soc., Chem. Commun.* **2001**, 1138−1139. (h) Pugh, V. J.; Hu, Q.-S.; Pu, L. *Angew. Chem., Int. Ed.* **2000**, *39*, 3638−3641. (i) Gong, L.-Z.; Hu, Q.-S.; Pu, L. *J. Org. Chem.* **2001**, *66*, 2358−2367. (j) Pugh, V. J.; Hu, Q.-S.; Zuo, X.-B.; Lewis, F. D.; Pu, L. *J. Org. Chem.* **2001**, *66*, 6136−6140.

(9) For a review on the enantioselective fluorescent recognition of chiral organic molecules, see: Pu, L. *Chem. Rev.* **2004**, *104*, 1687−1716.

(10) (a) Lin, J.; Hu, Q.-S.; Xu, M. H.; Pu, L. *J. Am. Chem. Soc.* **2002**, *124*, 2088−2089. (b) Xu, M.-H.; Lin, J.; Hu, Q.-S.; Pu, L. *J. Am. Chem. Soc.* **2002**, *124*, 14239−14246.

(11) (a) Brunner, H.; Schiessling, H. *Angew Chem., Int. Ed. Engl.* **1994**, *33*, 125−126. (b) Brunner, H.; Schiessling, H. *Bull. Soc. Chim. Belg.* **1994**, *103*, 119−126.

10.1021/jo049366a CCC: $27.50
Published on Web 08/24/2004

axially chiral binaphthyl units and four additional chiral carbon centers. These chiral elements may provide a good asymmetric environment for the desired enantioselective recognition. (2) The nitrogen atoms adjacent to the naphthalene fluorophores in these compounds can quench their fluorescence via a photoinduced electron transfer (PET) process.[12] Upon interaction of the nitrogen lone pair electrons with acidic protons, these macrocycles should show fluorescence enhancement by suppressing the PET quenching, leading to fluorescent signaling. (3) The tetrahydroxyl and tetraamine groups of these macrocycles are good hydrogen bond donors and acceptors. They should allow good binding with chiral carboxylic acids. We have found that these bisbinaphthyl macrocycles and their derivatives exhibit highly enantioselective fluorescent responses toward α-hydroxycarboxylic acids and α-amino acids. Herein, our studies of the fluorescence properties of the bisbinaphthyl macrocycles and derivatives and their applications in chiral recognition are reported. A portion of this work has been communicated earlier.[6]

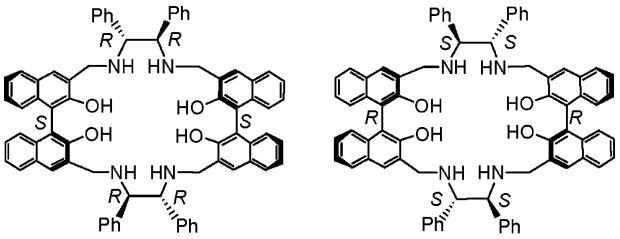

Results and Discussion

1. Synthesis of Macrocyclic and Acyclic Bisbinaphthyls. Scheme 1 shows the procedure developed by Brunner and Schiessling for the synthesis of the binaphthyl macrocycle (*S*)-**1**.[11] Condensation of the binaphthyl dialdehyde (*S*)-**2** with (*R*,*R*)-1,2-diphenylethane-1,2-diamine, (*R*,*R*)-**3**, in ethanol at reflux gave the macrocyclic Schiff base (*S*)-**4** in high yields. This macrocycle was then reduced with $NaBH_4$ in refluxing ethanol to give (*S*)-**1** in 98% yield. The enantiomer of this compound, (*R*)-**1**, was obtained by using (*R*)-**2** and (*S*,*S*)-**3** as the starting materials. It was also found that the mismatched chirality of (*R*)-**2** with (*R*,*R*)-**3** led to the formation of polymers rather than the macrocycle.[11]

We introduced conjugated substituents to the 6,6′-positions of the binaphthyl units of the macrocycle (*S*)-**1** to build compounds of more extended conjugation in order to improve the fluorescence property. Scheme 2 shows the construction of the bisbinaphthyl macrocycle with 6,6′-*p*-ethoxyphenyl substituents. The Suzuki coupling[13] of (*S*)-**5**[14] with *p*-ethoxyphenylboronic acid gave (*S*)-**6**,

SCHEME 1. Synthesis of the Bisbinaphthyl Macrocycle (*S*)-1

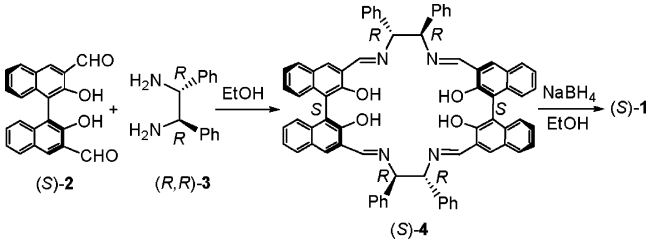

which was then converted to the chiral dialdehyde (*S*)-**7** by treatment with *n*-BuLi and DMF.[15] Condensation of (*S*)-**7** with the chiral diamine (*R*,*R*)-**3** gave a macrocyclic Schiff base which upon reduction with $NaBH_4$ produced the macrocycle (*S*)-**8** in 80% yield over the two steps. This compound contained four *p*-ethoxyphenyl groups at the 6,6′-positions of the two binaphthyls. Another 6,6′-substituted macrocycle (*S*)-**11** was prepared as shown in Scheme 3. The Heck coupling[16a,b] of (*S*)-**5** with styrene in the presence of Herrmann's catalyst gave (*S*)-**9**[16c] which was converted to the chiral dialdehyde (*S*)-**10**. Condensation of (*S*)-**10** with (*R*,*R*)-**3** followed by reduction with $NaBH_4$ produced (*S*)-**11** in 81% yield over the two steps.

The acyclic analogues of the bisbinaphthyl macrocycles were prepared for comparison in the subsequent fluorescent study. Schemes 4 and 5 show the use of the binaphthyl monoaldehydes (*R*)-**12** and (*S*)-**15** to generate the acyclic bisbinaphthyl compounds (*R*)-**14** and (*S*)-**16**. Compounds (*R*)-**12** and (*S*)-**15** were obtained in the preparation of (*R*)-**2** and (*S*)-**7**. Condensation of (*R*)-**12** with (*S*,*S*)-**3** in methylene chloride yielded the acyclic Schiff base (*R*)-**13** as reported by Kozlowski.[17] Reduction of (*R*)-**13** by $NaBH_4$ gave (*R*)-**14**. In the same way, (*S*)-**16** was obtained from the condensation of (*S*)-**15** with (*R*,*R*)-**3** followed by reduction.

2. NMR and UV Analyses of the Binaphthyl Compounds. The ^{1}H NMR spectra of the new macrocycles (*S*)-**8** and (*S*)-**11** were compared with that of (*S*)-**1**. In acetone-d_6, the *p*-ethoxyphenyl-substituted macrocycle (*S*)-**8** gave a doublet at δ 3.89 (J = 13.2 Hz, 4H) for one of the diastereotopic naphthylmethylene protons on the ring. The other naphthylmethylene proton signal overlapped with that of the methylene protons of the ethoxyl groups at δ 4.15 (m, 12 H). These signals were very close to what were observed at δ 3.73 and 4.12 (AB, 8H, J = 13.4 Hz) for the diastereotopic naphthylmethylene signals of (*S*)-**1**.[11b] The protons on the chiral carbon centers of (*S*)-**8** gave a singlet at δ 4.39 (s, 4H), and the methyl protons appeared at δ 1.42 (t, J = 6.9 Hz, 12 H). For the styryl-substituted macrocycle (*S*)-**11**, its naphthyl methylene signals appear at δ 3.88 and 4.08 (AB, J = 13.2 Hz, 8 H). Similar signals were observed for the two acyclic compounds (*R*)-**14** and (*S*)-**16**. In all of these compounds, no signals due to the hydroxyl and amine

(12) (a) Fox, M. A.; M. Chanon, M., Eds. *Photoinduced Electron Transfer. Parts A*−*D*; Elsevier: Amsterdam, 1988. (b) Bissell, R. A.; de Silva, A. P.; Gunaratna, H. Q. N.; Lynch, P. L. M.; Maguire, G. E. M.; McCoy, C. P.; Sandanayake, K. R. A. S. *Top. Curr. Chem.* **1993**, *168*, 223−264. (c) Bissell, R. A.; de Silva, A. P.; Gunaratna, H. Q. N.; Lynch, P. L. M.; Maguire, G. E. M.; Sandanayake, K. R. A. S. *Chem. Soc. Rev.* **1992**, *21*, 187−195. (d) Czarnik, A. W. *Acc. Chem. Res.* **1994**, *27*, 302−308.

(13) Suzuki, A. *J. Organomet. Chem.* **1999**, *576*, 147−168.

(14) Hu, Q.-S.; Vitharana, D.; Zheng, X.-F.; Wu, C.; Kwan, C. M. S.; Pu, L. *J. Org. Chem.* **1996**, *61*, 8370−8377.

(15) Cox, P. J.; Wang, W.; Snieckus, V. *Tetrahedron Lett.* **1992**, *33*, 2253−2256.

(16) (a) Heck, R. F. *Org. React.* **1982**, *27*, 345−390. (b) Herrmann, W. A.; Brossmer, C.; Öfele, K.; Reisinger, C.-P.; Priermeier, T.; Beller, M.; Fischer, H. *Angew. Chem., Int. Ed. Engl.* **1995**, *34*, 1844−1848. (c) Ostrowski, J. C.; Hudack, R. A.; Robinson, M. R.; Wang, S.; Bazan, G. C. *Chem. Eur. J.* **2001**, *7*, 4500−4511.

(17) DiMauro, E. F.; Kozlowski, M. C. *Org. Lett.* **2001**, *3*, 1641−1644.

SCHEME 2. Synthesis of the 6,6′-*p*-Ethoxyphenyl-Substituted Bisbinaphthyl Macrocycle (*S*)-8

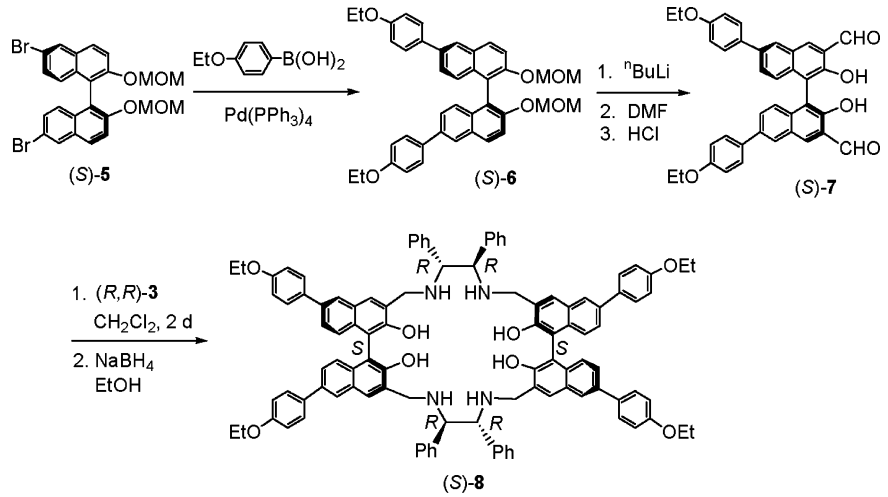

SCHEME 3. Synthesis of the 6,6′-Styryl-Substituted Bisbinaphthyl Macrocycles (*S*)-11

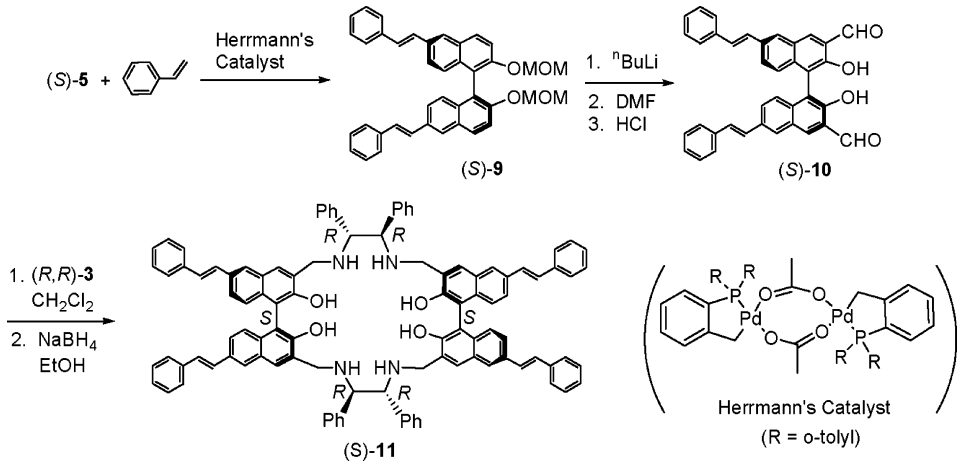

SCHEME 4. Synthesis of the Acyclic Bisbinaphthyl (*R*)-14

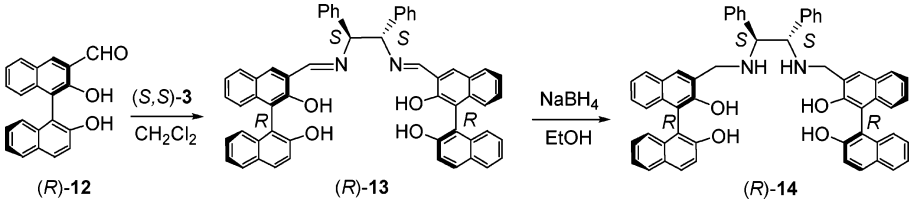

SCHEME 5. Synthesis of the Acyclic Bisbinaphthyl (*S*)-16

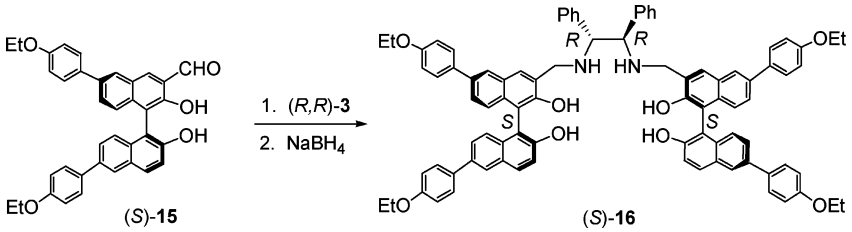

protons were observable. The structures of these compounds were confirmed by high-resolution mass spectroscopic analyses.

The UV spectra of the bisbinaphthyl compounds in benzene and methylene chloride are shown in Figures 1 and 2, respectively. From the unsubstituted compounds (*S*)-**1** and (*R*)-**14** to the 6,6′-substituted compounds (*S*)-**8**, (*S*)-**11**, and (*S*)-**16**, large red-shifts in the longest wavelength absorptions were observed. This is consistent with the increased conjugation in the 6,6′-substituted compounds. The substitution with the conjugated units also greatly increased absorbance. The absorption spectra of the macrocycles (*S*)-**1** and (*S*)-**8** are very close to those of their acyclic analogues (*R*)-**14** and (*S*)-**16**, respectively.

The UV spectra of (*S*)-**1** and (*R*)-**14** were compared with those of 2-naphthol and (*S*)-1,1′-bi-2-naphthol (BINOL)

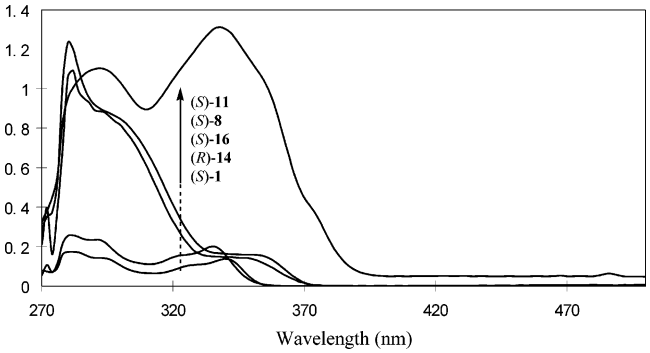

FIGURE 1. UV spectra of compounds (*S*)-**1**, (*S*)-**8**, (*S*)-**11**, (*R*)-**14**, and (*S*)-**16** in benzene (1.0×10^{-5} M).

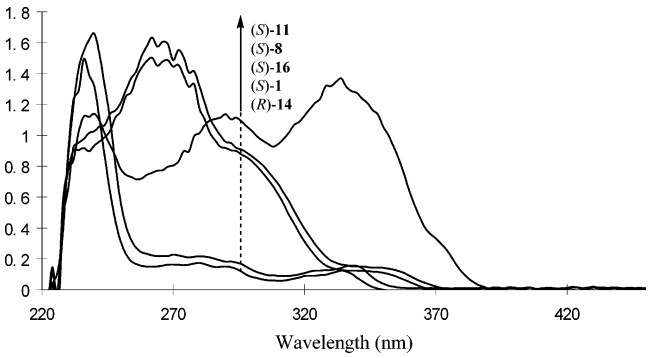

FIGURE 2. UV spectra of compounds (*S*)-**1**, (*S*)-**8**, (*S*)-**11**, (*R*)-**14**, and (*S*)-**16** in methylene chloride (1.0×10^{-5} M).

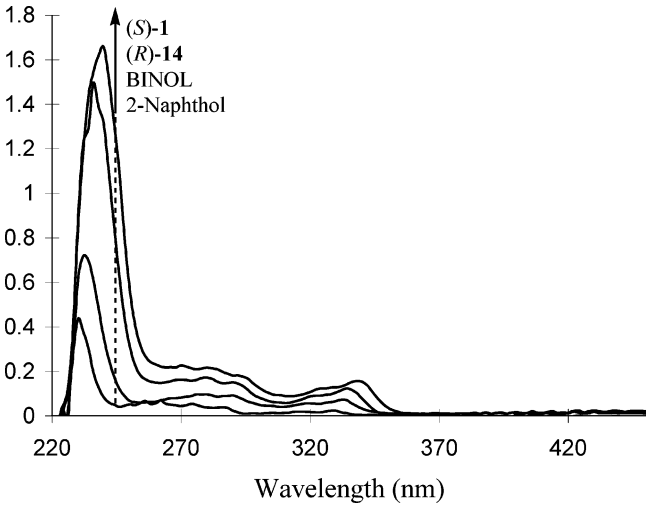

FIGURE 3. UV spectra of compounds (*S*)-**1**, (*R*)-**14**, 2-naphthol, and BINOL in methylene chloride (1.0×10^{-5} M).

in methylene chloride (Figure 3). Only a small red shift

at $\lambda_{max} \approx 230$ nm was observed going from 2-naphthol to BINOL and the bisbinaphthyl compounds, and the shape of the absorptions remained similar. This demonstrates that there is very little conjugation between the naphthalene rings in BINOL and the bisbinaphthyl compounds. There is also a small red-shift from BINOL to (*S*)-**1** in the longest wavelength absorption which could be attributed to the intramolecular hydrogen bonding between the hydroxyl groups and the amine nitrogens in (*S*)-**1**. This assumption is supported by the X-ray structure of (*S*)-**1** discussed in the next section. The UV absorption maxima and extinction coefficients of all the compounds are summarized in Table 1 of the supporting materials.

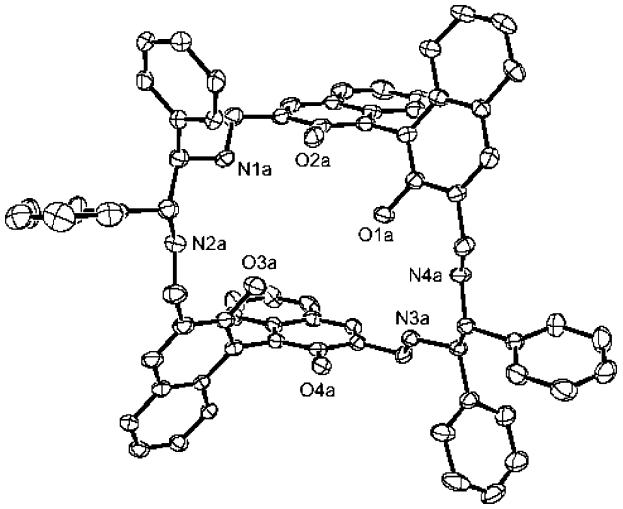

FIGURE 4. ORTEP drawing (30% ellipsoids) of (*S*)-**1**.

3. Molecular Structure of (*S*)-1. A single-crystal X-ray analysis of the chiral macrocycle (*S*)-**1** was conducted on a colorless crystal obtained from a deuterated acetone solution of (*S*)-**1**. The crystal was triclinic with the space group *P*1. Two independent molecules of slightly different conformation were found to exist in the unit cell of this molecule. Figure 4 shows the ORTEP drawing of one of those molecules. The central cavity of the macrocycle is flanked on two opposite sides by almost exactly parallel naphthol moieties separated by 7.65 Å. The long axes of the two groups are mutually perpendicular. In addition to the molecules of (*S*)-**1**, there are six molecules of deuterated acetone solvent molecules. Each of the macrocycles contains one of the solvent molecules sandwiched between the parallel naphthol units. This indicates that small molecules can be included inside the cavity of this macrocycle. The distances between the C atoms of acetone and naphthol range between 3.8 and 4.05 Å, indicating possible C−H···π interactions. All of the O atoms of the naphthol units are on the same side of the macrocycle. The macrocyle rings are stabilized by intramolecular O−H···N bonds, with the average O···N donor−acceptor distance of 2.68 Å in one molecule which is somewhat shorter than the corresponding distance of 2.75 Å in the other.

4. Fluorescence Spectra of the Unsubstituted Bisbinaphthyl Compounds (*S*)-1 and (*R*)-14. The fluorescence spectra of the bisbinaphthyl macrocycle (*S*)-**1** and the acyclic bisbinaphthyl (*R*)-**14** in methylene chloride are shown in Figure 5. Although these two compounds had almost identical UV spectra, they exhibited dramatic differences in emission. The macrocycle (*S*)-**1** gave dual fluorescence signals with a major emission

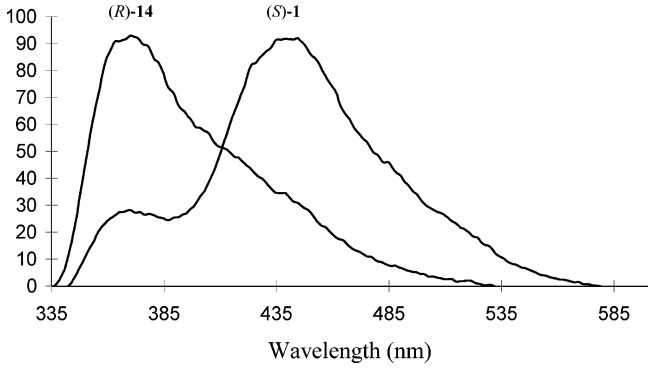

FIGURE 5. Fluorescence spectra of the macrocycle (*S*)-**1** and the acyclic compound (*R*)-**14** in methylene chloride (1.0×10^{-4} M, $\lambda_{exc} = 327$ nm).

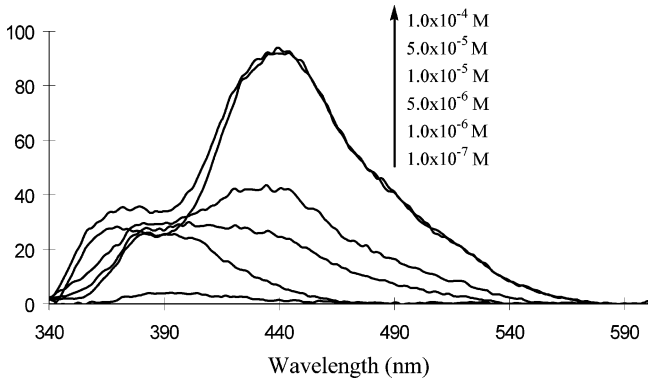

FIGURE 6. Concentration effect on the fluorescence of (*S*)-**1** in methylene chloride.

band at 439 nm (λ_{long}) and a small emission peak at 370 nm (λ_{short}) when excited at 327 nm. Its acyclic analogue (*R*)-**14**, however, gave a major emission at the short wavelength ($\lambda_{emi} = 371$ nm) with only low intensity shoulders in the long wavelength region.

To determine whether the long wavelength emission of (*S*)-**1** was due to an intramolecular transition or an intermolecular interaction, we studied the effect of concentration on its emission. Figure 6 compares the fluorescence spectra of (*S*)-**1** in methylene chloride in the concentration range of $10^{-7}-10^{-4}$ M. As the concentration of (*S*)-**1** decreased, the ratio of λ_{long} versus λ_{short} also decreased. At the concentrations below 10^{-6} M, only the emission at λ_{short} was observed. The UV spectra of (*S*)-**1** showed almost no change in the shape and position of the absorptions as the concentration of (*S*)-**1** increased from 10^{-7} to 10^{-4} M (see Figure 2 in the Supporting Information). These observations suggest that the long wavelength emission of the macrocycle should be due to the excimer emission of (*S*)-**1** formed between an excited molecule and that at ground state. The difference between the macrocycle (*S*)-**1** and the acyclic compound (*R*)-**14** in their fluorescence spectra demonstrates that they have different ability in forming the intermolecular excimers. It might be easier for the rigid macrocycle to achieve a stronger intermolecular interaction because it may be less solvated than the flexible acyclic compound.

The fluorescence spectra of (*S*)-**1** and (*R*)-**14** in benzene were similar to those in methylene chloride. We measured the fluorescence spectra of (*S*)-**1** in a mixed solvent

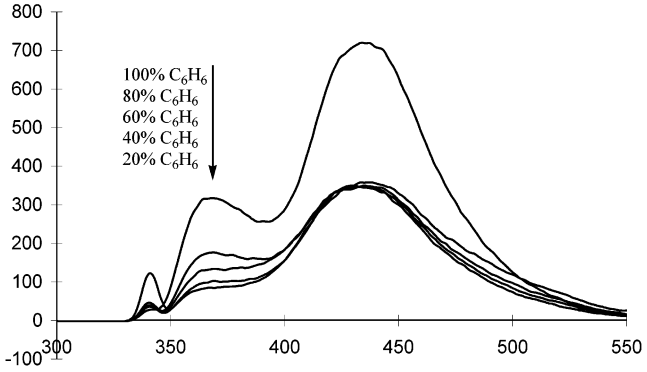

FIGURE 7. Fluorescence spectra of (*S*)-**1** in benzene/2-propanol solutions (1.0×10^{-4} M).

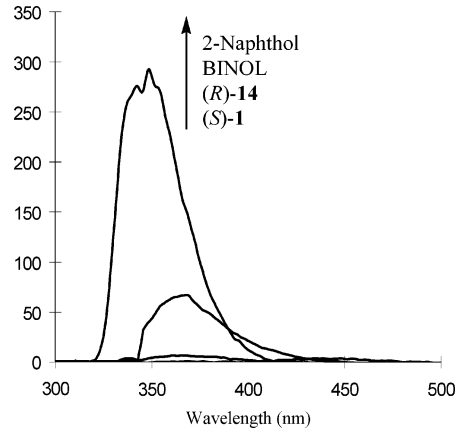

FIGURE 8. Fluorescence spectra of 2-naphthol, BINOL, (*S*)-**1**, and (*R*)-**14** in methylene chloride (2.0×10^{-6} M, $\lambda_{exc} = 274$, 278, 305, and 305 nm, respectively).

of benzene and 2-propanol. As shown in Figure 7, addition of 2-propanol to a benzene solution of (*S*)-**1** (1.0×10^{-4}) initially led to the reduction of the emissions at both λ_{short} and λ_{long}. After more than 20% of 2-propanol was added, there was almost no change for the excimer emission while the emission at λ_{short} decreased continuously. This indicates that the intermolecular interaction for the excimer of (*S*)-**1** may not be through hydrogen bonds. Little change in the UV spectra was observed for (*S*)-**1** in the mixed benzene/2-propanol solutions. As shown by the X-ray structure of (*S*)-**1**, all of the hydroxyl groups of (*S*)-**1** are involved in intramolecular hydrogen bonding with the amine nitrogens. This makes (*S*)-**1** less likely to form intermolecular hydrogen bonds both in the ground state as well as in the excited state. No intermolecular hydrogen bonds were found in the solid-state structure of (*S*)-**1**.

The fluorescence spectra of the macrocycle (*S*)-**1** and the acyclic compound (*R*)-**14** were compared with those of 2-naphthol and BINOL. As shown in Figure 8, 2-naphthol and BINOL had much stronger fluorescence intensity (by ca. 2 orders of magnitude) than (*S*)-**1** and (*R*)-**14** at 2.0×10^{-6} M even though the light absorption of the bisbinaphthyl compounds was much stronger. The fluorescence signals of both (*S*)-**1** and (*R*)-**14** are close to the baseline in Figure 8. This is because the fluorescence of (*S*)-**1** and (*R*)-**14** is largely quenched by their nitrogen lone pair electrons via the PET process. The lower

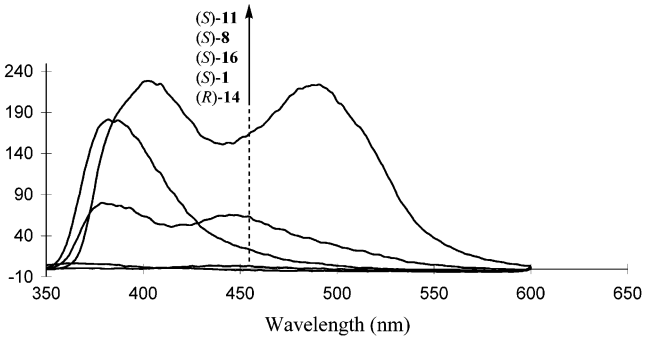

FIGURE 9. Comparison of the fluorescence spectra of the 6,6′-substituted compounds (*S*)-**8**, (*S*)-**11**, and (*S*)-**16** with those of the unsubstituted compounds (*S*)-**1** and (*R*)-**14** in methylene chloride (2.0×10^{-6} M).

fluorescence intensity of BINOL than 2-naphthol can be attributed to the rotation around the 1,1′-bond of BINOL, which could facilitate the nonradiative decay of its excited state. The emission maxima of 2-naphthol and BINOL were at 349 and 368 nm, respectively, close to λ_{short} of the macrocycle (*S*)-**1** and the acyclic compound (*R*)-**14**.

5. Fluorescence Spectra of the 6,6′-Substituted Bisbinaphthyl Compounds (*S*)-8, (*S*)-11, and (*S*)-16. The fluorescence spectra of the 6,6′-substituted bisbinaphthyl compounds (*S*)-**8**, (*S*)-**11**, and (*S*)-**16** are compared with those of the unsubstituted compounds (*S*)-**1** and (*R*)-**14** in methylene chloride at 2.0×10^{-6} M (Figure 9). As shown in Figure 9, introduction of the 6,6′-conjugated substituents to the binaphthyl compounds not only caused red shifts for the emission maxima, but also enhanced the fluorescence intensity by about 2 orders of magnitude.[10b] Similar to (*S*)-**1**, the 6,6′-substituted macrocycles (*S*)-**8** and (*S*)-**11** gave intense excimer emissions at 445 and 491 nm, respectively, when excited at 305 nm. They also had short wavelength emissions at 379 and 403 nm, respectively. When the concentrations of these two macrocycles were reduced, the excimer emissions relative to the short wavelength emissions were greatly reduced. The flexible acyclic compound (*S*)-**16** gave mainly the short wavelength emission at 382 nm, similar to (*R*)-**14**. When the solvent was changed from methylene chloride to benzene, the long wavelength emissions of (*S*)-**8** and (*S*)-**11** were greatly reduced and the short wavelength emissions became the predominate signals.

6. Enantioselective Fluorescent Recognition of α-Hydroxycarboxylic Acids Using the Unsubstituted Macrocycles (*S*)- and (*R*)-1 and the Acyclic Compound (*R*)-14. We studied the interaction of (*S*)- and (*R*)-**1** with mandelic acid, a chiral aromatic α-hydroxycarboxylic acid. In our study of the fluorescent recognition in this and later sections, the enantioselectivities were obtained by measuring the changes in the fluorescence intensity of the sensors corresponding to the two enantiomers of the substrate at the same concentration. The fluorescence intensities were not normalized with respect to the corresponding absorptions because these results are more useful for the future high-throughput screening measurement. Therefore, the obtained enantioselectivity of these sensors in this paper does not necessarily reflect the differences in the quantum yields of the sensors when treated with the two enantiomers of the substrate.

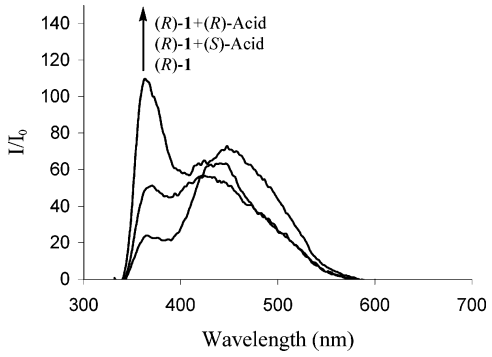

FIGURE 10. Fluorescence spectra of (*R*)-**1** (1.0×10^{-4} M in CH_2Cl_2/2% DME) in the presence of (*R*)- and (*S*)-mandelic acid (0.02 M) (λ_{exc} = 327 nm).

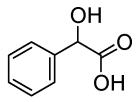

mandelic acid

Figure 10 shows the fluorescence spectra of (*R*)-**1** in methylene chloride in the presence of (*R*)- and (*S*)-mandelic acid. The methylene chloride solution contained 2% dimethoxyethylene (DME) in order to improve the solubility of mandelic acid. The two emission bands of the chiral macrocycle responded differently to the acid. The emission at λ_{long} showed small change in intensity when treated with the two enantiomers of mandelic acid. However, large changes were observed at λ_{short}. The two enantiomers of mandelic acid enhanced the fluorescence of the macrocycle at λ_{short} very differently. This enantioselective fluorescent response corresponds to an ef of 3.2 [ef: enantiomeric fluorescence difference ratio = $(I_R - I_0)/(I_S - I_0)$]. (*R*)-Mandelic acid enhanced the fluorescence of (*R*)-**1** to a much greater extent than (*S*)-mandelic acid.

The interaction of the macrocycle with mandelic acid in benzene (containing 2% DME) was also studied and the results were communicated earlier.[6] When the macrocycle (*S*)-**1**, the enantiomer of (*R*)-**1**, was treated with the enantiomers of mandelic acid in benzene, very different fluorescence responses from those in methylene chloride were observed. (*S*)-Mandelic acid greatly enhanced the excimer emission of (*S*)-**1** at λ_{long}, but (*R*)-mandelic acid only led to a small enhancement. At λ_{short} of (*S*)-**1**, (*S*)-mandelic acid generated a small enhancement while (*R*)-mandelic acid quenched the fluorescence slightly. The enantioselective fluorescence response of (*S*)-**1** toward the two enantiomers of mandelic acid at λ_{long} was extremely high with an ef value greater than 12. At a lower concentration of (*S*)-**1**, e.g., 10^{-5} and 10^{-6} M, the enantioselectivity was greatly reduced.

As described above, the fluorescence of the sensor responded toward mandelic acid in very different ways in benzene or methylene chloride. The major enantioselectivity was observed at the short wavelength emission in methylene chloride but at the excimer emission in benzene.

The fluorescence enhancement of (*S*)-**1** at λ_{long} in the presence of 5.0×10^{-3} to 2.0×10^{-2} M of (*R*)- and (*S*)-

mandelic acid in benzene demonstrates that although (*R*)-mandelic acid did not significantly enhance the fluorescence of (*S*)-**1** in the measured concentration range, (*S*)-mandelic acid generated over 2-fold fluorescence enhancement.[6] The enantiomer (*R*)-**1** was also interacted with (*R*)- and (*S*)-mandelic acid under the same conditions as above. A mirror image relationship with the responses of (*S*)-**1** was observed. That is, (*R*)-mandelic acid greatly enhanced the fluorescence of (*R*)-**1** at λ_{long}, and (*S*)-mandelic acid caused little change. This confirmed the enantioselective fluorescent responses of the bisbinaphthyl macrocycles toward mandelic acid.

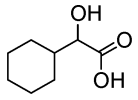

hexahydromandelic acid

The macrocycle (*S*)-**1** was also used to recognize hexahydromandelic acid, an aliphatic α-hydroxycarboxylic acid.[6] We observed that while the (*S*)-acid enhanced the intensity of (*S*)-**1** significantly at λ_{long} in benzene (2% DME), the (*R*)-acid almost did not change the fluorescence. This is the same as the responses of (*S*)-**1** toward mandelic acid except that the magnitude of the fluorescent enhancement (≤1.8-fold) was smaller in the case of hexahydromandelic acid.

The fluorescence intensity of (*S*)-**1** at λ_{long} was found to be linearly related to the enantiomeric composition of mandelic acid and hexahydromandelic acid. Thus, these bisbinaphthyl macrocycles can be used as highly enantioselective fluorescent sensors for the recognition of both aromatic and aliphatic α-hydroxycarboxylic acids.

We studied the fluorescence property of the acyclic compound (*S*)-**14** in the presence of (*R*)- and (*S*)-mandelic acid in benzene. Although large fluorescence enhancements were observed at λ_{short}, the enantioselectivity was very small (ef = 1.1−1.4) (see Figure 5 in the Supporting Information).

7. Enantioselective Fluorescent Recognition of α-Hydroxycarboxylic Acids and α-Amino Acid Derivatives Using the 6,6′-Substituted Bisbinaphthyl Macrocycles (*S*)-8, (*S*)-11 and the Acyclic Compound (*S*)-16. a. Enantioselective Fluorescent Recognition of Mandelic Acid. The 6,6′-substituted compounds were used for the fluorescent recognition of mandelic acid in methylene chloride solution. Figure 11 gives the fluorescence spectra of (*S*)-**8** in the presence of (*R*)- and (*S*)-mandelic acid. Large fluorescence enhancement of the 6,6′-*p*-ethoxyphenyl substituted macrocycle (*S*)-**8** at λ_{short} was observed when treated with mandelic acid. In the meantime, the excimer emission at λ_{long} was either quenched or unchanged. The fluorescence enhancement at λ_{short} was enantioselective with an ef of ca 2. The effect of the mandelic acid concentration on the fluorescence enhancement was studied and the results are plotted in Figure 12. The error bars in the plot were obtained by four independent measurements. This fluorescence enhancement at λ_{short} of (*S*)-**8** is similar to that of the unsubstituted macrocycle (*S*)-**1** in methylene chloride as shown in Figure 10 except that the fluorescence intensity of (*S*)-**8** was much stronger and its fluorescence measurements could be conducted at concentrations of 2 orders of magnitude lower, i.e., 10^{-6} M versus 10^{-4} M. Mandelic acid also enhanced the fluorescence of the acyclic compound (*S*)-**16** in methylene chloride, but almost no enantioselectivity was observed.

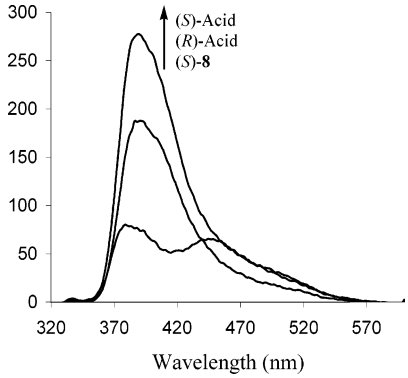

FIGURE 11. Fluorescence spectra of the 6,6′-*p*-ethoxyphenyl bisbinaphthyl macrocycle (*S*)-**8** (2.0×10^{-6} M in CH_2Cl_2/0.4%DME) in the presence of (*R*)- and (*S*)-mandelic acid (4.0×10^{-3} M) ($\lambda_{exc} = 305$ nm).

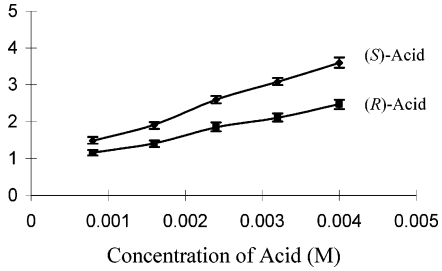

FIGURE 12. Fluorescence enhancement at λ_{short} of (*S*)-**8** (2.0×10^{-6} M in CH_2Cl_2/0.4%DME) versus concentration of (*R*)- and (*S*)-mandelic acid ($\lambda_{exc} = 305$ nm).

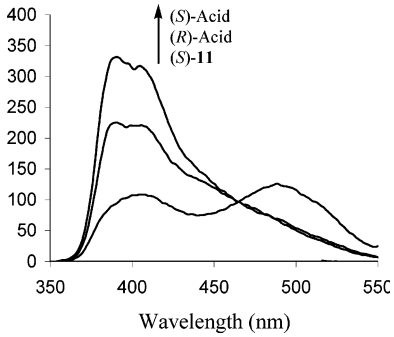

FIGURE 13. Fluorescence spectra of the 6,6′-styryl-substituted macrocycle (*S*)-**11** (2.0×10^{-6} M in CH_2Cl_2/0.4%DME) with (*R*)- and (*S*)-mandelic acid (4.0×10^{-3} M) ($\lambda_{exc} = 305$ nm).

The 6,6′-styryl-substituted macrocycle (*S*)-**11** behaved similarly as (*S*)-**8** when treated with the enantiomers of mandelic acid in methylene chloride (Figure 13). Both (*R*)- and (*S*)-mandelic acid quenched the excimer emission of the macrocycle at λ_{long} and enhanced at λ_{short}. The fluorescence enhancement at λ_{short} is enantioselective with an ef of ca 2. The effect of the concentration of mandelic acid on the fluorescence enhancement at λ_{short} (380 nm) was shown in Figure 14.

We also studied the interaction of the 6,6′-substituted bisbinaphthyls with mandelic acid in *benzene*. Although the acyclic compound (*S*)-**16** showed the expected fluo-

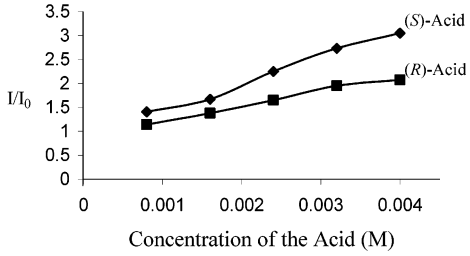

FIGURE 14. Fluorescent enhancement at λ_{short} of (*S*)-**11** (2.0×10^{-6} M in CH_2Cl_2/0.4% DME) in the presence of (*R*)- and (*S*)-mandelic acid ($\lambda_{exc} = 305$ nm).

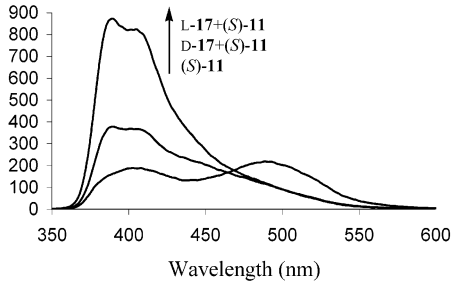

FIGURE 15. Fluorescence spectra of (*S*)-**11** (2.0×10^{-6} M in CH_2Cl_2/0.4% DME) in the presence of D- and L-**17** (4.0×10^{-3} M) ($\lambda_{exc} = 336$ nm).

rescent enhancement, we were surprised to find that both (*R*)- and (*S*)-mandelic acid quenched the fluorescence of the macrocycles. The solution remained clear when the macrocycles were treated with the acid. Thus, precipitation was not the cause of the fluorescence reduction. It is unclear at this stage what contributed to the fluorescence quenching in benzene.

b. Enantioselective Fluorescent Recognition of the N-Protected Phenyl Glycine 17. The unsubstituted macrocycles (*R*)- and (*S*)-**1** were used to recognize N-protected α-amino acids, and highly enantioselective fluorescent responses to a few substrates were detected.[18] We also studied the fluorescence responses of the 6,6′-substituted macrocycles (*S*)-**8** and (*S*)-**11** to D- and L-**17** in the presence of the N-protected phenylglycine **17**.

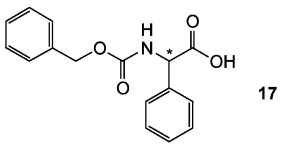

17

N-Benzyloxycarbonylphenylglycine

Because of the much stronger fluorescent signals of these compounds with 6,6′-conjugated substituents, their fluorescence studies were conducted at concentrations of 2 orders of magnitude lower (10^{-6} M versus 10^{-4} M) than the unsubstituted (*R*)- and (*S*)-**1**.[18] Figures 15 and 16 show the fluorescence change of (*S*)-**11** when treated with D- and L-**17**. The error bars in Figure 16 were obtained by three independent measurements. Figures 17 and 18 show the fluorescence change of (*S*)-**8** when treated with D- and L-**17**. The chiral amino acid quenched the excimer emissions of both macrocycles but enhanced their short

(18) Lin, J.; Li, Z.-B.; Zhang, H.-C.; Pu, L. *Tetrahedron Lett.* **2004**, *45*, 103−106.

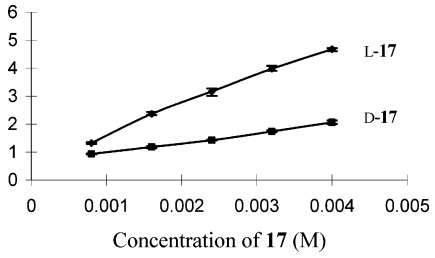

FIGURE 16. Fluorescence enhancement at λ_{short} of (*S*)-**11** (2.0×10^{-6} M in CH_2Cl_2/0.4% DME) with D- and L-**17** ($\lambda_{exc} = 336$ nm, ef at $\lambda_{short} = 3.5-7$).

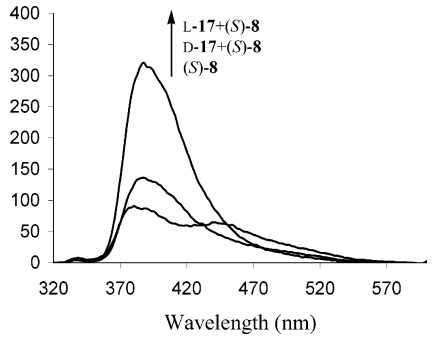

FIGURE 17. Fluorescence spectra of (*S*)-**8** (2.0×10^{-6} M in CH_2Cl_2/0.4% DME) in the presence of D- and L-**17** (4.0×10^{-3} M) ($\lambda_{exc} = 305$ nm).

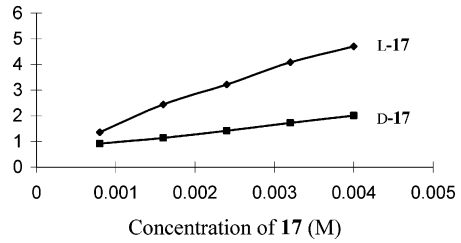

FIGURE 18. Fluorescence enhancement at λ_{short} of (*S*)-**8** (2.0×10^{-6} M in CH_2Cl_2/0.4% DME) with D- and L-**17** ($\lambda_{exc} = 305$ nm, ef at $\lambda_{short} = 3.7-10$).

wavelength emissions. Both of the macrocycles exhibited very high enantioselectivity in their fluorescent responses to the amino acid. The observed ef values were up to 10. These compounds are useful as highly enantioselective fluorescent sensors for the recognition of this amino acid derivative.

Summary

A series of optically active macrocyclic and acyclic bisbinaphthyls have been synthesized and characterized. The structure of one of the bisbinaphthyl macrocycles has been established by a single-crystal X-ray analysis. The UV and fluorescence spectra of these chiral compounds in various solvents and at different concentrations are studied. Formation of excimers is observed for the macrocyclic bisbinaphthyl compounds. Introduction of conjugated substituents to the 6,6′-positions of the binaphthyl units in the macrocycles leads to greatly amplified fluorescence signals. Using the 6,6′-substituted bisbinaphthyl macrocycles in place of the unsubstituted macrocycles allows a 2 orders of magnitude reduction in

the sensor concentration for the fluorescence measurements. These macrocycles have exhibited highly enantioselective fluorescent enhancements in the presence of chiral α-hydroxycarboxylic acids and N-protected α-amino acids. They are useful as fluorescent sensors for chiral recognition. The macrocycles show much greater enantioselectivity in the substrate recognition than their acyclic analogues.

Experimental Section

Preparation and Characterization of (*S*,*S*)-6,6′-Bis(4-ethoxyphenyl)-2,2′-bis-methoxymethoxy[1,1′]binaphthalenyl, (*S*)-6. To a round-bottom flask were added (*S*)-**5** (2.00 g, 3.75 mmol), $Pd(PPh_3)_4$ (320 mg, 0.28 mmol), THF (50 mL), 4-ethoxyphenylboronic acid (1.38 g, 8.31 mmol), and aqueous potassium carbonate solution (1 M, 9.4 mL). After being degassed by freeze−pump−thaw for three times, the reaction mixture was heated under nitrogen at reflux for 2 d. The solvent was evaporated, and the residue was extracted with methylene chloride. The methylene chloride solution was washed with water and brine and dried with Na_2SO_4. After filtration and removal of the solvent, the residue was purified by column chromatography on silica gel eluted with CH_2Cl_2/hexanes (30/70) to give (*S*)-**6** (2.15 g) as a white solid in 93% yield. ^{1}H NMR ($CDCl_3$, 300 MHz): δ 1.41 (t, J = 7.2 Hz, 6H), 3.16 (s, 6H), 4.06 (q, J = 7.2 Hz, 4H), 4.99 (d, J = 6.9 Hz, 2H), 5.09 (d, J = 6.9 Hz, 2H), 6.93 (s, 2H), 6.96 (d, J = 2.1 Hz, 2H), 7.24 (d, J = 9.0 Hz, 2H), 7.44 (dd, J = 2.1, 9.0 Hz, 2H), 7.58−7.62 (m, 6H), 7.98 (d, J = 9.0 Hz, 2H), 8.02 (d, J = 1.5 Hz, 2H). ^{13}C NMR ($CDCl_3$, 75 MHz): δ 14.8, 55.8, 63.5, 95.2, 114.8, 117.7, 121.1, 124.9, 125.8, 126.0, 128.1, 129.5, 130.2, 132.8, 133.3, 136.4, 152.6, 158.4. Mp: 88−91 °C. $[\alpha]_D$ = +112.2 (c = 1.14, CH_2Cl_2).

Preparation and Characterization of (*S*)-6,6′-Bis(4-ethoxyphenyl)-2,2′-dihydroxy[1,1′]binaphthalenyl-3,3′-dicarbaldehyde, (*S*)-7, and (*S*)-6,6′-Bis(4-ethoxyphenyl)-2,2′-dihydroxy[1,1′]binaphthalenyl-3-carbaldehyde, (*S*)-15. (1) Preparation of (*S*)-6,6′-Bis(4-ethoxyphenyl)-2,2′-bis-methoxymethoxy[1,1′]binaphthalenyl-3,3′-dicarbaldehyde (A) and (*S*)-6,6′-Bis(4-ethoxyphenyl)-2,2′-bis-methoxymethoxy[1,1′]binaphthalenyl-3-carbaldehyde (B). To a stirred solution of (*S*)-**6** (1.00 g, 1.63 mmol) in Et_2O (40 mL) was added *n*-BuLi (4.3 mL, 6.8 mmol, 1.61 M in hexane) at room temperature under nitrogen. The stirring continued for 2 h, and the resulting mixture was cooled to 0 °C. DMF (0.57 mL, 7 mmol) was slowly added, and the suspension was then warmed to room temperature. After an additional 4 h, saturated aqueous NH_4Cl was added to quench the reaction. Methylene chloride was added to extract several times. The combined organic layer was washed with water and brine and dried over Na_2SO_4. After filtration and removal of solvent, the residue was purified by flash column chromatography on silica gel eluted with hexane containing 12−16% ethyl acetate to give **A** (475 mg, 43%) and **B (**129 mg, 12%) as yellow solids. For **A**: ^{1}H NMR ($CDCl_3$, 300 MHz): δ 1.45 (t, J = 7.2 Hz, 6H), 2.93 (s, 6H), 4.10 (q, J = 7.2 Hz, 4H), 4.73 (d, J = 6 Hz, 2H), 4.78 (d, J = 6 Hz, 2H), 7.02 (d, J = 8.7 Hz, 4H), 7.25−7.32 (m, 2H), 7.63(d, J = 8.7 Hz, 4H), 7.69 (m, 2H), 8.21 (m, 2H), 8.65 (s, 2H), 10.57 (s, 2H). For **B**: ^{1}H NMR ($CDCl_3$, 300 MHz): δ 1.42 (t, J = 7.2 Hz, 6H), 3.05 (s, 3H), 3.20 (s, 3H), 4.10 (q, J = 7.2 Hz, 4H), 4.69 (d, 6 Hz, 1H), 4.80 (d, 6 Hz, 1H), 5.09 (d, 6.9 Hz, 1H), 5.18 (d, 6.9 Hz, 1H), 6.96−7.02 (m, 4H), 7.25−7.32 (m, 2H), 7.52−7.65 (m, 7H), 8.02−8.05 (m, 2H), 8.18 (m, 1H), 8.61 (s, 1H), 10.61 (s, 1H).

(2) Preparation of (*S*)-7. Compound **A** (330 mg, 0.49 mmol) was dissolved in methylene chloride (50 mL) and combined with trifluoroacetic acid (0.5 mL, 6.4 mmol). After the mixture was stirred for 2 h, the organic layer was washed with water several times and brine and dried over Na_2SO_4. The solvent was then evaporated, and the residue was purified by flash column chromatography on silica gel eluted with hexane containing 18−22% ethyl acetate to give (*S*)-**7** (260 mg) as a yellow solid in 91% yield. ^{1}H NMR ($CDCl_3$, 300 MHz): δ 1.43 (t, J = 6.9 Hz, 6H), 4.08 (q, J = 6.9 Hz, 4H), 6.94−7.01 (m, 4H), 7.24−7.29 (m, 2H), 7.54−7.58 (m, 4H), 7.63−7.67 (m, 2H), 8.10−8.12 (m, 2H), 8.36 (s, 2H), 10.12 (s, 2H), 10.60 (s, 2H). ^{13}C NMR ($CDCl_3$, 75 MHz): δ 15.1, 63.9, 115.3, 116.7, 122.7, 125.6, 127.0, 128.3, 128.4, 130.7, 132.7, 136.5, 137.3, 138.9, 153.8, 159.0, 197.1. Mp: 144−147 °C. $[\alpha]_D$ = 110.0 (c = 0.64, CH_2Cl_2). HRMS: calcd for $C_{38}H_{30}O_6$ 582.2073, found 582.2057. Anal. Calcd for $C_{38}H_{30}O_6$: C, 78.33; H, 5.19. Found: C, 78.49; H, 5.32.

(3) Preparation of (*S*)-15. By using the same procedure as for the preparation of (*S*)-**7**, compound **B** was hydrolyzed to give (*S*)-**15** as a yellow solid in 91.7% yield. ^{1}H NMR ($CDCl_3$, 300 MHz): δ 1.46 (m, 6H), 4.13 (m, 4H), 5.01 (br s, 1H), 7.00−7.76 (m, 13H), 7.95−8.08 (m, 2H), 8.19−8.21 (m, 1h), 8.47 (s, 1H), 10.27 (s, 1H), 10.70 (s, 1H). ^{13}C NMR (acetone-d_6, 75 MHz): δ 14.5, 63.4, 63.5, 114.0, 115.0, 115.2, 117.4, 119.1, 119.2, 123.3, 125.3, 125.8, 126.8, 128.1, 128.2, 128.6, 129.6, 129.8, 130.3, 132.5, 133.3, 133.4, 135.4, 136.7, 137.0, 138.7, 153.4, 154.6, 158.8, 159.2, 198.0. Mp: 146−149 °C. $[\alpha]_D$ = +102.9 (c = 0.71, CH_2Cl_2). HRMS: calcd for $C_{37}H_{30}O_5$ 554.2093, found 554.2112. Anal. Calcd for $C_{37}H_{30}O_5$: C, 80.12; H, 5.45. Found: C, 79.96; H, 5.64.

Preparation and Characterization of the 6,6′-*p*-Ethoxyphenyl-Substituted Bisbinaphthyl Macrocycle, (*S*)-8. The dialdehyde (*S*)-**7** (300 mg, 0.51 mmol) and (*R*,*R*)-1,2-diphenylethane-1,2-diamine (109.2 mg, 0.51 mmol) [(*R*,*R*)-**3**] were dissolved in CH_2Cl_2 (20 mL) and stirred for 2 d at room temperature under nitrogen. After the solvent was removed, the crude product was purified by passing through a short silica gel column eluted with methylene chloride to give the macrocyclic Schiff base as a yellow solid. The Schiff base was then dissolved in ethanol (40 mL) and combined with $NaBH_4$ (55 mg, 1.45 mmol). The resulting reaction mixture was heated under nitrogen at reflux for 4 h to form a clear colorless solution. After removal of the solvent, methylene chloride (30 mL) and HCl (0.2 N, aq, 30 mL) were added, and the solution was stirred for 2 h. The organic layer was separated and washed with saturated aq $NaHCO_3$, water, and brine. The solution was dried over $MgSO_4$ and then passed through a short silica gel column eluted with CH_2Cl_2/acetone (1:5). The product was further purified by recrystallization from CH_2Cl_2 and ethanol to give (*S*)-**8** as a white solid in 80% overall yield. ^{1}H NMR (acetone-d_6, 300 MHz): δ 1.42 (t, J = 6.9 Hz, 12H), 3.89 (d, J = 13.2 Hz, 4H), 4.15 (m, 12H), 4.39 (s, 4H), 6.94−7.03 (m, 12H), 7.16−7.29 (m, 12H), 7.36−7.44 (m, 12H), 7.55−7.64 (m, 12H), 7.94 (s, 4H). ^{13}C NMR (acetone-d_6, 75 MHz): δ 15.1, 52.2, 64.0, 69.6, 115.6, 117.1, 125.5, 126.3, 127.7, 128.2, 128.3, 128.6, 129.1, 129.2, 129.3, 133.8, 134.1, 135.4, 140.6, 155.2, 159.3. Mp: 222 °C dec. $[\alpha]_D$ = −15.9 (c = 0.11, CH_2Cl_2). HRMS: calcd for $C_{104}H_{93}N_4O_8$ (MH^+) 1525.6988, found 1525.6998. Anal. Calcd for $C_{104}H_{92}N_4O_8$: C, 81.86; H, 6.08; N, 3.67. Found: C, 81.92; H, 6.35; N, 3.40.

Preparation and Characterization of (*S*,*S*)-2,2′-Bis-methoxymethoxy-6,6′-distyryl[1,1′] binaphthalenyl, (*S*)-9. To a round-bottom flask were added (*S*)-**5** (2.00 g, 3.76 mmol), Herrmann's catalyst [*trans*-di(μ-acetato)bis[*o*-(di-*o*-tolylphosphino)benzyl]dipalladium(II)] (165 mg, 0.17 mmol), sodium acetate (1.40 g, 16.9 mmol), and DMF (100 mL). Then styrene (2.64 mL, 22.6 mmol) was added, and the resulting mixture was heated at 130 °C under nitrogen for 2 d. After bering cooled to room temperature, the reaction mixture was diluted with water and extracted with methylene chloride. The solvent was evaporated, and the residue was purified by column chromatography on silica gel eluted with CH_2Cl_2/hexanes (30/70) to give (*S*)-**9** (1.62 g) as a white solid in 74% yield. ^{1}H NMR ($CDCl_3$, 300 MHz): δ 3.22 (s, 6H), 5.05 (d, J = 6.9 Hz, 2H), 5.16 (d, J = 6.9 Hz, 2H), 7.15−7.23 (m, 4H), 7.27−7.32 (m, 4H), 7.40 (t, J = 7.5 Hz, 4H), 7.53 (s, 2H), 7.59(d, J =

7.5 Hz, 4H), 7.64 (d, J = 9.0 Hz, 2H), 7.95 (s, 2H), 8.01 (d, J = 9.0 Hz, 2H). ^{13}C NMR ($CDCl_3$, 75 MHz): δ 56.2, 95.5, 117.9, 121.6, 124.4, 126.3, 126.7, 127.0, 127.8, 128.7, 129.0, 129.8, 130.4, 133.4, 133.9, 137.7, 153.2. Mp: 184−186 °C. $[\alpha]_D$ = +427.6 (c = 0.63, CH_2Cl_2).

Preparation and Characterization of (*S*)-2,2′-Dihydroxy-6,6′-distyryl[1,1′]binaphthalenyl-3,3′-dicarbaldehyde, (*S*)-10. (1) Preparation of (*S*,*S*)-2,2′-Bis-methoxymethoxy-6,6′-distyryl[1,1′]binaphthalenyl-3,3′-dicarbaldehyde (C). A procedure similar to the preparation of **A** was applied to make **C** from (*S*)-**9**. After general workup, the crude product was purified by column chromatography on silica gel eluted with hexane containing 12−16% ethyl acetate to give **C** as a yellow solid in 60% yield. ^{1}H NMR ($CDCl_3$, 300 MHz): δ 2.95 (s, 6H), 4.75 (d, J = 6.9 Hz, 2H), 4.80 (d, J = 6.9 Hz, 2H), 7.22−7.45 (m, 12H), 7.58−7.61 (m, 4H), 7.72−7.75 (m, 2H), 8.12 (s, 2H), 8.65 (s, 2H), 10.61 (s, 2H). ^{13}C NMR ($CDCl_3$, 75 MHz): δ 57.1, 100.7, 125.9, 126.5, 126.7, 127.3, 127.4, 128.1, 128.3, 128.8, 129.2, 130.3, 130.4, 132.1, 135.4, 136.1, 136.8, 154.1, 190.6. Mp: 86−89 °C. $[\alpha]_D$ = +260.6 (c = 0.42, CH_2Cl_2). **(2) Preparation of (*S*)-10.** The procedure used for the hydrolysis of **C** to give (*S*)-**10** was the same as the hydrolysis of **A** in the preparation of (*S*)-**7**. After general workup, the crude product was purified by column chromatography on silica gel eluted with hexane containing 12−16% ethyl acetate to give (*S*)-**10** as a yellow solid in 34% yield. The low yield may be due to the side reaction of the styryl double bonds under the strong acidic conditions, and higher yields were observed at smaller scale reactions. ^{1}H NMR ($CDCl_3$, 300 MHz): δ 7.10−7.30 (m, 8H), 7.32−7.39 (m, 4H), 7.51−7.53 (m, 4H), 7.65−7.68 (m, 2H), 7.99 (s, 2H), 8.33 (s, 2H), 10.12 (s, 2H), 10.62 (s, 2H). ^{13}C NMR ($CDCl_3$, 75 MHz): δ 116.96, 122.65, 125.55, 126.86, 127.96, 128.16, 128.18, 128.46, 128.68, 129.04, 129.59, 133.99, 137.19, 137.34, 138.61, 154.21, 197.07. Mp: 163−166 °C. $[\alpha]_D$ = +59.8 (c = 0.37, CH_2Cl_2). HRMS: calcd for $C_{38}H_{26}O_4$ 546.1831, found 546.1802.

Preparation and Characterization of the 6,6′-Styryl-Substituted Bisbinaphthyl Macrocycle (*S*)-11. The same procedure as for the preparation of (*S*)-**8** was applied to synthesize (*S*)-**11** from (*S*)-**10**. After separation with a short silica gel column and recrystallization from methylene chloride and ethanol, (*S*)-**11** was obtained as a white solid in 81% overall yield. ^{1}H NMR (acetone-d_6, 300 MHz): δ 3.88 (d, J = 13.2 Hz, 4H), 4.08 (d, J = 13.2 Hz, 4H), 4.37 (s, 4H), 6.89−6.92 (m, 4H), 7.18−7.40 (m, 40H), 7.46−7.51 (m, 8H), 7.58−7.61 (m, 8H), 7.82 (s, 4H). ^{13}C NMR (acetone-d_6, 75 MHz): δ 51.6, 69.1, 116.9, 123.6, 125.6, 126.6, 127.1, 127.2, 127.5, 127.6, 128.5, 128.6, 128.7, 128.9, 129.1, 132.0, 133.9, 138.0, 140.1, 155.2. Mp: 227 °C dec. $[\alpha]_D$ = +108.7 (c = 0.13, CH_2Cl_2). HRMS: calcd for $C_{104}H_{85}N_4O_4$ (MH^+) 1453.6565, found 1453.6495. Anal. Calcd for $C_{104}H_{84}N_4O_4$: C, 85.92; H, 5.82; N, 3.85. Found: C, 86.06; H, 5.80; N, 3.91.

Preparation and Characterization of the Acyclic Compound (*R*)-14. By using a procedure similar to the preparation of (*R*)-**1**, a 2:1 mixture of (*R*)-**12** and (*S*,*S*)-**3** was converted to (*R*)-**14**. After separation with a short silica gel column and recrystallization from methylene chloride and ethanol, (*R*)-**14** was obtained as a white solid in 88% overall yield. ^{1}H NMR (acetone-d_6, 300 MHz): δ 3.93 (d, J = 13.8 Hz, 2H), 4.09 (d, J = 13.8 Hz, 2H), 4.20 (s, 2H), 6.92−6.98 (m, 4H), 7.02−7.26 (m, 20H), 7.62 (s, 2H), 7.70−7.73 (m, 2H), 7.77−7.82 (m, 4H). ^{13}C NMR (acetone-d_6, 75 MHz): δ 49.98, 67.37, 114.51, 115.46, 118.67, 122.85, 122.96, 124.54, 125.16, 125.97, 126.16, 127.27, 127.39, 128.12, 128.14, 128.28, 128.66, 128.85, 129.23, 129.30, 134.27, 134.76, 140.27, 153.13, 154.93. Mp: 167−171 °C. $[\alpha]_D$ = +19.2 (c = 0.53, CH_2Cl_2). HRMS: calcd for $C_{56}H_{45}N_2O_4$ (MH^+) 809.3374, found 809.3359.

Preparation and Characterization of the Acyclic Compound (*S*)-16. By using a procedure similar to the preparation of (*S*)-**8**, a 2:1 mixture of (*S*)-**15** and (*R*,*R*)-**3** was converted to (*S*)-**16**. After separation with a short silica gel column and recrystallization from methylene chloride and ethanol, (*S*)-**16** was obtained as a white solid in 79% overall yield. ^{1}H NMR (acetone-d_6, 300 MHz): δ 1.40−1.46 (m, 12H), 3.99(d, J = 13.2 Hz, 2H), 4.06−4.15 (m, 8H), 4.21 (d, J = 13.2 Hz, 2H), 4.30 (s, 2H), 6.98−7.28 (m, 24H), 7.34−7.39 (m, 2H), 7.52−7.74 (m, 12H), 7.82−7.85 (m, 2H), 8.01−8.06 (m, 4H). ^{13}C NMR (acetone-d_6, 75 MHz): δ 14.53, 50.00, 63.42, 66.94, 114.65, 114.97, 115.06, 115.58, 119.04, 125.04, 125.23, 125.29, 125.46, 125.94, 127.40, 127.63, 128.12, 128.33, 128.68, 129.22, 129.48, 129.54, 133.24, 133.52, 133.57, 133.60, 135.14, 135.31, 140.23, 153.03, 154.98, 158.72, 158.80. Mp: 185−188 °C. $[\alpha]_D$ = +177.0 (c = 0.58, CH_2Cl_2). HRMS: calcd for $C_{88}H_{77}N_2O_8$ (MH^+) 1289.5674, found 1289.5682. Anal. Calcd for $C_{88}H_{76}N_2O_8$: C, 81.96; H, 5.94; N, 2.17. Found: C, 81.89; H, 5.95; N, 2.38.

Preparation of Samples for Fluorescence Measurements. Materials: The sensors were purified by column chromatography and recrystallization and then stored in a refrigerator. The enantiomers of mandelic acid were purchased from Aldrich and recrystallized from methanol. The amino acid derivatives were purchased from Advanced Chemtech. All of the solvents were HPLC grade. The benzene and CH_2Cl_2 stock solutions of the sensors were freshly prepared for each measurement. A 0.01 M stock solution of mandelic acid or the amino acid was freshly prepared by using solvents (benzene or CH_2Cl_2) containing 1% (v) DME. DME was added to improve the solubility of the acid. For the fluorescence enhancement study, a sensor solution was mixed with the mandelic acid solution at room temperature in a 5 mL volumetric flask and diluted to the desired concentration. The resulting solution was allowed to stand at room temperature for 2−4 h before the fluorescence measurement.

Acknowledgment. Support of this work from the National Institutes of Health (R01GM58454/R01EB002037-05) is gratefully acknowledged.

Supporting Information Available: Additional UV, fluorescence, and excitation spectra. This material is available free of charge via the Internet at http://pubs.acs.org.

JO049366A